Magnet Design of Toroidal Field Coils for the UWMAK-Tokamak Systems

R.W. Boom, R.W. Moses, Jr., and W.C. Young

March 1976

UWFDM-158

To be published in *Nuclear Engineering and Design.*

FUSION TECHNOLOGY INSTITUTE

UNIVERSITY OF WISCONSIN

MADISON WISCONSIN

Magnet Design of Toroidal Field Coils for the UWMAK-Tokamak Systems

R.W. Boom, R.W. Moses, Jr., and W.C. Young

Fusion Technology Institute
University of Wisconsin
1500 Engineering Drive
Madison, WI 53706

http://fti.neep.wisc.edu

March 1976

UWFDM-158

To be published in *Nuclear Engineering and Design.*

Magnet Design of Toroidal Field Coils

for the UWMAK-Tokamak Systems

by

R. W. Boom, R.W. Moses, Jr. and W.C. Young

Fusion Technology Program
Nuclear Engineering Department
University of Wisconsin-Madison
U.S.A.

To be published in Nuclear Eng. and Design

Abstract

The design of toroidal field coils for the UWMAK series of Tokamak reactor designs is described. These are cryogenically stable coils cooled in liquid helium to 4.2 K. Each individual turn of composite conductor of TiNb plus matrix conductor is epoxied into a groove in a thin disk structure. The magnet is divided into 12, 18 or 24 sectors; each sector is comprised of 15-20 thin disks which are spaced and bolted together to form a rigid structure with all disk surfaces exposed to cooling. The overall shape of each "D" magnet sector is chosen so that only constant tension forces are present. Bending forces do occur but only near transition sections from the D to the central straight section of each coil. This method of rigid mounting should be compared with loose "jelly-roll" windings on a central coil form, a more typical magnet fabrication technique. The design procedure is for the composite conductor TiNb plus copper (or aluminum) to be mounted in stainless steel (or aluminum alloy) disks. Full stability is obtained for strains less than 0.2% for steel support and less than 0.4% for aluminum supports based on stress-strain resistivity experiments in progress. The use of high purity aluminum conductor and high strength aluminum alloy structure reduces costs significantly dependent only on the orderly development of new aluminum TiNb composite conductors. The amount of TiNb is conservatively chosen to carry full current at 5.2 K although operation at 4.2 K is planned and full recovery to the superconducting state could be obtained with full current wire quantities selected at 4.3 K. This conservative choice doubles the amount of TiNb used at 8 tesla but provides an extra temperature rise of $\Delta T = 0.9$ K above expected usual temperature excursions. Magnet safety and protection is based on the natural mutual coupling of many coils which are closely coupled to each other. If one coil loses current, the other coils increase their currents in order to keep the flux as constant as possible. The uncoupled flux and companion field energy would be discharged by a high voltage power supply temporarily set to discharge the one bad coil. Such sub-division and partial energy removal requires that there be substantial subdivision of coils into many separate dewars, so that problems can be isolated. An expression for the magnetic forces on sectioned toroidal field coils is given in closed form and is used to compute the shape of a specific coil. Data obtained here are shown to be in good agreement with those given by more complex procedures. The most severe structural design requirement is based on simultaneous loss of current in two adjacent sectors. The remaining sectors attempt to straighten out into a solenoid which compresses structure between coils except beside the bad coil or coils where tension might exist. Such current loss in two adjacent sectors is considered an extremely unlikely occurrence since the discharge procedure mentioned above takes place in less than one minute so that simultaneous refers to a one minute overlap. Because of such rapid amelioration of the causes of current change and flux motion, no temperatures can exceed room temperature during the orderly shutdown of one or two coils. In general, the study illustrates that fully stable magnets using composite conductors should be engineered without major uncertainties according to straightforward scientific concepts. While subsequent designs will undoubtedly include improvements there is no reason to expect that superconductivity implies venturesome unknown TF coil performance.

I. Introduction

Certain basic aspects of the design of superconducting toroidal field magnets must be considered before all others in order to qualify the Tokamak fusion power reactor as a viable source of commercial electrical energy. This paper outlines these crucial aspects and discusses the reasons that the authors feel make them of primary importance. Design procedures are described which address the problems uncovered. Possible solutions are detailed for many of the problems, along with a discussion of the reliability and safety achieved by each choice.

II. Design Constraints

The following list of design related requirements or constraints will be accepted as fact for the purpose of the subsequent discussion. Relaxation of certain portions of these requirements could possibly lower projected costs or lead to more easily attainable solutions but until further study shows that such relaxation is feasible they will remain as constraints.

1. Vertical field coils are required to maintain the plasma in equilibrium and for economic reasons alone these vertical field coils must be placed inside the windings of the toroidal field magnets.
2. Given the present state of the art, joints which can be disconnected and reconnected as a part of a routine maintenance procedure are not possible in stabilized superconductors and the associated

structure. Therefore, the vertical field coils will have to be constructed in place inside the toroidal field magnets.

3. The degree of reliability required is such that the toroidal field magnets must not fail in a way that would require their removal during the expected life of the plant.
4. The method of construction must permit 100% inspection of all components at all stages of construction to assure the necessary reliability.
5. In order to reduce the cost of the toroidal field magnets it is necessary to minimize the structural mass in these magnets.
6. Any design must provide for full and unfailing cryogenic stability for the superconductor-stabilizer composite conductor.

The following design discussion is independent of the choice of magnetic field. However, it should be noted that higher fields require more structure (mass $\sim B^2/2\mu_o$) and more structural space and that strain sensitive superconductors, such as Nb_3Sn, may, in addition, require even more structure in order to limit strains.

III. Constant Tension Structural Design

In order to minimize structural mass the average principal stress in the structure must be maximized. According to the virial theorem of Classius,[1] Levi[2] showed that the mass of structure required to confine a magnetic field is proportional to the stored energy. For idealized one dimensional stresses:

$$M_t - M_c \geq \frac{\rho}{\sigma_w} E, \tag{1}$$

where M_t = mass of structure in tension

M_c = mass of structure in compression

$E_w = \int_{\text{all space}} dv \int HdB$ = total magnetic energy

ρ = structure density

σ_w = uniform stress in all structure.

It is therefore desirable to minimize the total mass by minimizing the total mass in compression since $M_{total} = M_t + M_c$ and since additionally any material in compression must be equaled by a corresponding excess structure under tension. File, Mills, and Sheffield[3] have proposed "D" shaped toroidal field coils which are in one dimensional tension without compression and without bending stresses. The ideal shaped "D" magnet is a unique shape which is tangent to the vertical inner straight section at the intersection point at H_{R1}, Fig. 1. The ideal "D" is rarely the one finally chosen for a Tokamak design, however, since it is not always the best enclosure of a volume determined by many other factors. In the UWMAK-I design[4] the height H_{max} chosen for the toroidal field magnets was lower than the ideal "D" while the UWMAK-III

design[5] the opposite is true. Deviations from the ideal shape add more structure but are generally less costly than a larger ideal "D" which would encompass the internal portion of the reactor.

Several finite element analyses of proposed "D" shaped toroidal field magnets[6,7] have revealed unexpected bending stresses primarily in the region where the curved inner portion of the D joins the vertical straight inner leg. A major reason for these bending stresses is the inaccurate determination of the shape of the magnet due to errors in the mathematical model used. One of these errors is created by the field perturbations or ripples which are created by having a finite number of coils rather than a continuous toroidal winding. File[8] and Wang[9] have described iteration procedures to correct for these perturbations while Moses and Young[10] have derived an approximate but very accurate analytical expression for magnetic forces on sectored toroidal coils. Their derivation can be summarized as follows. The toroidal field magnet is divided into N coils each carrying a total current I. The conductors are distributed in circular, square or rectangular cross sections that are the same at all locations around the D. Conductor coordinates are defined as in Fig. 1. Neglecting field ripple due to the sectored form of the toroid, the field approximation is

$$B_\theta \simeq \mu_o NI/2\pi R. \tag{2}$$

The corresponding radial force per unit length on a coil is

$$f_{\ell} \simeq \mu_o NI^2/4\pi R \tag{3}$$

where the force is averaged over the coil cross section, see Fig. 3. Next, corrections to Eq. (3) are developed to account for dividing the toroid into a relatively small number of sectors.

The first correction is attributed to the so-called toroidal curvature illustrated in Fig. 2. A set of straight parallel conductors is shown carrying current normal to the surface of the drawing. The magnetic field can be expressed precisely for this configuration[11] and forces on the inside and outside conductors are well approximated by

$$f_{\ell 1} \simeq \frac{\mu_o NI^2}{4\pi R}\,(1-1/N) \tag{4}$$

and

$$f_{\ell 2} \simeq \frac{\mu_o NI^2}{4\pi R}\,(1+1/N) \tag{5}$$

respectively. In each case the force is perpendicular to the conductor and directed away from the high field region. Throughout this discussion N is the total number of discrete coils. Each coil may have many closely packed turns, but from the standpoint of force computation we treat it as a circular conductor of radius c or a square of width w. Rectangular coils could be considered similarly.

The conductors of Fig. 2 bear a resemblance to conductors on the toroidal midplane in Fig. 1, $\phi = 0$ and π. A correction for the conductor curvature will be added in the following paragraphs; however, Eqs. (4) and (5) can be modified to account for conductor orientation anywhere

around the coil. These are replaced by the single expression

$$f_{\ell} \simeq \frac{\mu_o N I^2}{4\pi R} \left(1 + \frac{1}{N} \cos \phi\right). \tag{6}$$

The validity of Eq. (6) for values of ϕ between 0 and π is more easily demonstrated by example than by rigorous proof as will be seen later.

To obtain the solenoidal curvature correction, consider first a long straight solenoid of radius ρ with coil to coil spacing s. If the surface were a thin uniform sheet of conductor, the energy stored per segment would be

$$E_c = \frac{\mu_o I^2}{2} \frac{\pi \rho^2}{s} \tag{7}$$

Equation (7) is volume related, while the use of discrete coils adds a surface correction. In the case of round conductors of radius c, Eq. (7) is replaced by[10]

$$E_c \simeq \frac{\mu_o I^2}{2} \left(\frac{\pi \rho^2}{S} + \rho \ell n (0.2044\ s/c)\right). \tag{8}$$

The force per unit length of conductor on a solenoid of discrete coils is then

$$f_{\ell} = \frac{1}{2\ \rho} \frac{\partial E_c}{\partial \rho} \simeq \frac{\mu_o I^2}{2s} \left[1 + \frac{s}{2\pi\rho} \ell n(0.2044\ s/c)\right] \tag{9}$$

Since the surface effect terms in Eqs. (8) and (9) are generated by field perturbations close to the conductor, the force in Eq. (9) is related to the radius of curvature ρ and the magnet does not need to be strictly circular. As an example it could have the D shape of Fig. 1.

The next step is to add the effects of toroidal curvature in Eq. (6) and solenoidal curvature in Eq. (9) to get a corrected version of Eq. (3)

$$f_{\ell} \simeq \frac{\mu_o NI^2}{4\pi R} \left[1 + \frac{1}{N}\left(\cos\phi + \frac{R}{\rho} \ell n \frac{1.284R}{cN}\right)\right] . \tag{10}$$

For a square coil cross section of width w one may replace c with 0.593 w. Equation (10) was shown to be accurate to within 0.1% for 18 circular coils. This and other tests are discussed in greater detail in reference 10.

The radius of curvature is proportional to R in the 1/R field approximation

$$\frac{\rho}{R} = \frac{\rho_2}{R_2} . \tag{11}$$

When ρ/R is corrected for field ripple it takes the form

$$\frac{\rho}{R} = \left[\frac{\rho_2}{R_2}\left(1 + \frac{1}{N}\right) - \frac{1}{N} \ell n \frac{R}{R_2}\right]/\left(1 + \frac{1}{N}\cos\phi\right). \tag{12}$$

Note that while the shape and the proportions of the magnet cross

section, and the properties of the materials used determine the size of the required cross section they do not change the expression for the radius of curvature of the center line of the "D" shape. Reference 10 also presents design curves and equations which enable the designer to choose the necessary parameters of an appropriate "D" shape without going through the calculations.

As an example of the efficacy of this procedure let us examine the design of the toroidal field magnets proposed for a Tokamak Experimental Power Reactor by the design team at Argonne National Laboratory.[6,9] This example using 16 coils is chosen since they presented a three-dimensional stress analysis for the final shape of the constant tension "D" and along the perimeter of this magnet the variation of the stress in the outer skin is shown to be small. As expected, their work shows large variations in stress for both the circular coil and the constant tension "D" based on a 1/R internal field variation. They chose instead of a 1/R internal field variation an average internal field variation at each coil of $1/(\alpha_1 + \alpha_2 R + \alpha_3 R^2)$. When the expression for the local radius of curvature ρ is set proportional to the reciprocal of the field variation one obtains

$$\rho = (\beta_1 + \beta_2 R + \beta_3 R^2) = \pm\left[1 + \left(\frac{dz}{dR}\right)^2\right]^{3/2} \Big/ \frac{d^2 z}{dR^2} . \qquad (13)$$

The coefficients, β_1, β_2 and β_3 for a given trial are obtained by a least squares fit to the numerical values of field distribution calculated from the shape produced by the previous trial. The procedure

starts with the fields generated by the coil shape produced by the usual 1/R field variation for a non-sectored toroid.

Five iterations led to the several values shown in Table 1 for the desired ratio $R_1/R_2 = 0.237$.

Using the design equations from Reference 10 based on the analytical expression in Eq. (12) and using a linear variation in 1/N to obtain coefficients for 16 coils, the following formulas are obtained:

$$R_1/R_2 = 1.000-2.253(\rho_2/R_2) + 2.440(\rho_2/R_2)^2-1.497(\rho_2/R_2)^3+0.417(\rho_2/R_2)^4 \quad (14)$$

$$H_{R_1}/R_2 = 0.000-0.2000(\rho/R_2)+2.057(\rho_2/R_2)^2-1.748(\rho_2/R_2)^3+0.560(\rho_2/R_2)^4 \quad (15)$$

$$H_{max}/R_2 = 0.000+1.026(\rho_2/R_2)-0.232(\rho_2/R_2)^2+0.053(\rho_2/R_2)^3-0.008(\rho_2/R_2)^4 \quad (16)$$

$$R_{H_{max}}/R_2 = 1.000-1.062(\rho_2/R_2)+0.560(\rho_2/R_2)-0.186(\rho_2/R_2)^3+0.033(\rho_2/R_2)^4 \quad (17)$$

Setting $R_1/R_2 = 0.237$ and solving the above formulas gives the values shown in Table 1. Although the Argonne design showed relatively little bending of the shape reached after five iterations there is nevertheless some bending producing compression on the outside at the top, $\phi = 90°$, and tension on the outside at the top of the inner leg. The University of Wisconsin solution is seen from Table 1 to be extremely close to

the Argonne solution and the differences are all such as to reduce the already small bending stresses present in the Argonne design.

Table 1

A Comparison of Iterative and Approximate Analytical Solutions for $R_1/R_2 = 0.237$

Ratio Evaluated	From Argonne Iterative Solution	From U.W. Approximate Analytical Solution	% Difference
ρ_2/R_2	--	0.6362	--
H_{R_1}/R_2	0.3362	0.3468	+3.2
H_{max}/R_2	0.5752	0.5712	-0.7
$R_{H_{max}}/R_2$	0.5053	0.5085	+0.6

A second source of error which creates bending stresses in a constant tension design occurs at the interface between the straight inner leg of the magnet and the most sharply curved portion of the "D" which connects to it. A constant thickness cross section cannot produce a transition here without some bending stress since the position of the resultant load in the cross section of the straight portion is not the same as in the curved portions. It should be recalled that the position of the resultant load is at midthickness only if the thickness is very small in comparison to the radius of curvature of a curved member under radial loading. As an example, Young[12] gives an expression for the circumferential hoop stress σ_2 in a thick-walled circular ring under a radial body force which varies from δ_b at the inner radius to zero at the outer radius. For a case where the thickness of the ring is one-fifth the outside radius

and Poisson's ratio is taken as 0.3, the expression for circumferential hoop stress becomes

$$\sigma_2 = \delta_b a[1.814-2.667\ r/a + 1.188(r^2/a^2)+0.043(a^2/r^2)] \qquad (18)$$

where a is the outer radius and r the radius at which σ_2 is evaluated. Integrating this expression for δ_2 over the wall thickness reveals that the resultant circumferential tensile force is positioned a distance of 0.025 times the wall thickness from the midthickness position. The maximum circumferential tensile stress on the inside surface of the ring is 1.17 times the average tensile stress. The purpose of this brief example is to call attention to the fact that the transition from the curved inner position of the "D" to the straight inner leg is not going to be entirely free of bending and shear stresses for magnets of finite thickness.

When one also considers that the ideal "D" may not be the economic choice for the shape of a toroidal field magnet, the transition from the curved free standing portion to the radially supported inner leg becomes even more difficult to design without using excessive quantities of structural material. Two entirely different designs[5,13] are presented in the UWMAK-II and UWMAK-III studies since the deviations from the ideal shape were in opposite directions.

IV. Constant Tension Manufactured Solid Disk (Not Wound) Magnets

The case for designing magnets as manufactured assemblies of conductors mounted in a structure as compared to layer wound or pancake wound magnets

is outlined in the following list of design considerations.

1. Motion between loose wound magnet components during charging and discharging may overheat turns. A large fusion magnet would have to be wound either under considerable tension around an inner structural form, or else be encapsulated solidly inside a binder such as epoxy.

   If the magnet windings are pretensioned on a form, no concave or straight portion of the form is possible and the varying radius of curvature of the "D" shaped magnet makes pretensioning extremely difficult. The extra mass of the internal form needed to withstand the winding loads is in the wrong location to assist in carrying magnetic loadings. It cannot be removed after winding since in a "D" shape the pretensioned windings are not in equilibrium by themselves.

   If the solidly encapsulated form of a wound magnet were used it would be virtually impossible to assure sufficient cooling to provide full cryogenic stability.

   The solid former method of construction allows the designer full freedom to modify the size and shape of the magnet where desired and in fact provides for attachment of each former to the central core. No restrictions are present on the sense of the curvature of the conductor. Conductor grooves which are concave outward are permitted if field shaping by such means is necessary or if assembly techniques require such grooves for economy of construction. Bolting through the interior of the windings is possible only with the solid former

type of construction. This permits the magnet itself to carry a larger share of any out-of-plane loading which may occur if one coil loses current. A full analysis of the response of this type of construction to such an accident is detailed in the UWMAK-II report.[13]

2. The need for 100% inspection and testing of all components at all stages of construction dictates against the wound magnets. A wound pancake would be extremely difficult to handle and test. In a layer wound magnet the addition of each layer modifies those layers previously placed. Therefore testing must be continuous and success is not assured until the final turns are completed, fastened, and tested.

   The solid former method of construction proposed in all three UWMAK designs, in which conductors are insulated and bonded into machined or forged grooves in a properly shaped "D" shaped disk, permits inspection and testing, even in liquid helium before final assembly into a magnet.

3. The problem of voltage breakdown of the electrical insulation between the conductors and the structure during a rapid discharge of the energy from a toroidal field magnet poses problems to all designs. In the solid former method all structure would no doubt be at ground potential which aggravates the problem. Numerous solutions are being studied and appear to be no more difficult or costly than those associated with wound magnets. This significant problem is treated further in the safety discussion below.

IV-a. Conductor Design for Imbedded TF Coils in Solid Disk Formers

Complete cryogenic stability is assumed to be the only viable design at this time. Cryogenically stable conductors are composite conductors of superconductor and normal metal arranged so that the total transport current can be carried in the normal metal for a long period of time without excess temperature rises. It is not our intention to review all aspects of cryogenic stability here; the reader is referred to the extensive literature of the 1960's.[14,15,16,17] It should be noted, however, that the subject has received new emphasis with the recent recognition that large magnets must be cryogenically stable. Most of the superconducting magnet development for the past ten years has dealt with cryogenically unstable magnets which use conductors with inadequate amounts of copper and surface cooling for steady state stability. However, this unstable conductor work is useful for TF coil design in that it has introduced multifilamentary conductors and has explored ac loss phenomena. A major task now is to reinstitute cryogenic stability development projects by assimilating the appropriate accomplishments from unstable magnet developments and then proceeding to the design problems of large stable magnets.

A typical cross section for a UWMAK disk conductor is shown in Fig. 3. The copper cross section; the number, size and location of the TiNb filaments; the selection of material for the disk; and the method of mounting the conductor on the disk are all determined by stability criteria with derating for extra reliability. Briefly, these design

determinations are:

1. Stainless-steel structure is used for the UWMAK-I and II disk material because it is non-magnetic and not brittle at low temperature. The maximum stress level used is 60,000 psi, a derating from 90,000 psi yield stress. The strain at 60,000 psi is 0.002 (0.2%). The amount of steel is found approximately from the tensile load requirement, $T = \bar{B}I\rho$, where $\bar{B}$ is the average local field, I is the total current per disk and ρ is the local radius of curvature. Following Eq. (12) local radii of curvature ρ are varied along the D structure so that T is constant for a constant tension TF coil, as verified by finite element stress analysis.

2. The superconductor TiNb is chosen because it can survive strains of 1% or more without degradation and because it can produce the maximum field required, 8.7 tesla, at 4.2 K. At this writing in 1976 the only alternative, Nb_3Sn, degrades at any strain level and at 0.2% strain would be of questionable value. Work by Cornish, Zbasnik and Pattee[18] should help clarify the possibility of use of Nb_3Sn in large magnets within the next few years; certainly the case for Nb_3Sn will be decided before the year 2000 when commercial Tokamak reactors are scheduled for construction.

Another factor in favor of TiNb is that its lower magnetic field appears to be sufficient for Tokamak reactors. Boom, Conn, and Lue[19] in a recent study shows with present scaling laws, in comparison to a 5000 MW_{th} low field TiNb Tokamak reactor, that a higher field Nb_3Sn Tokamak would be larger, produce more power and require much higher first wall neutron loading. Kulcinski[20] has shown that first wall elements probably require 20-30 days to replace. Therefore the cost of changing the first wall seems to more than negate any other advantages of higher

magnetic field units. In fact, as of 1976, it appears that the first wall radiation problem would dictate a low field (TF) TiNb coil system.

3. The conductor sketch in Fig. 3 shows a composite surface layer of TiNb in copper which is soldered to a larger backing strip of copper. The cryogenic stability criteria with extra allowance is interpreted here to be that no TiNb filament shall exceed 5.2 K for either of two cases: (1) all the current is in the copper or (2) part of the current is carried by the superconductor filaments while partially resistive. The problem then reduces to calculating the temperature of the most poorly cooled filament of TiNb under the most adverse, but normally occurring conditions. Previously[4] we had added all of these extremes in temperature together, even though they cannot all occur simultaneously. The surface temperature drop taken was $\Delta T_1 = 0.5$ K to the helium at 0.4 W/cm^2 when all the current is in the copper, $\Delta T_2 \leq 0.25$ K between the surface and the filament for heat conduction through the copper and $\Delta T_3 \leq 0.25$ K for the temperature drop from the filament surface to its center. Then for all combinations of temperature extremes we chose enough TiNb superconductor to carry the total transport current at T = 5.2 K, even though that temperature was higher than possible.

Hilal[21] has improved on this model by finding the filament temperature, and filament current capacity, as a continuous function of the fraction of the current in the substrate (copper) varying from 1 to 0. If there is always excess superconductor current capacity then the fraction of current in TiNb can increase towards recovery from a normal excursion, causing the fraction of current in the copper to decrease. In this way Hilal showed that recovery is assured, that is

cryogenic stability is assured, if there is enough superconductor to carry the total current at T = 4.3 K for the UWMAK-II configuration shown in Fig. 3. If only 4.2 K quantities are used then he showed that recovery will stop when TiNb carries 90% of the current and copper 10% which then becomes the stable local operating point. This may be one of the explanations for the fact that it is so difficult to get magnets to carry "short sample current," a long time goal for designers.

We use Hilal's results now as a gage for our conservative choice; TiNb amounts are still maintained at the 5.2 K quantity with a safety factor of $\Delta T = 0.9$ K. Initiation of normal regions would require a $\Delta T = 1$ K in both copper and TiNb for current to move from the TiNb and be shared with the copper. Recovery will take place much easier because there is excess TiNb. This reliability is obtained by including extra TiNb; about twice as much TiNb at 5.2 K is required compared to 4.3 K, see Fig. 4.[22] However the cost difference is small compared to structural and copper costs which remain unchanged.

4. Each filament should be less than a critical diameter so that filaments do not generate too much heat while current sharing with the copper matrix. It is known[23] that the rate of heat transfer from a filament is

$$w = 8\pi k[\bar{T}-T_o] \tag{19}$$

where k is 0.1 W/mK for TiNb, $\bar{T}$ is the average filament temperature and T_o is the filament surface temperature. Therefore $\bar{T}$ per filament would be less than 4.3 K for the above example and the number of filaments

would be found from n = P/w, where P is the total power to be dissipated. Hilal[21] has improved on Eq. (19) by calculating the exact temperature distribution in a filament and then the accurate current capacity. The principle remains the same and implies that using more small filaments is better than a few larger ones. We typically select an order of magnitude more filaments than Eq. (19) would require as another extra reliability factor.

5. The rectangular copper + TiNb conductor is bonded into spiraling grooves formed in each surface of the disk with epoxy-fiberglass. We assume the fibers will assist in locating the conductor in the groove and that the epoxy will fill the interstices and provide the bonding action.

Magnet protection must include fast enough energy removal circuits so that the epoxy temperature cannot get too high, for example, above 300 K. This might occur during a catastrophic disaster, such as an inadvertent rupture of the vacuum helium vessel which would initiate immediate shutdown procedures. Such considerations lead to an epoxy thickness requirement. Should the copper temperature rise to 300 K so suddenly that the steel is still at low temperature then the copper expands ($\Delta L/L \cong 0.0033$) relative to the steel. In order to do no more damage than extrude epoxy the epoxy edge channel should be something like 0.01 cm thick or greater.

V. Aluminum Stabilizer and Structure

The most advanced TF coil conductor we have considered is an aluminum matrix TiNb composite conductor supported by 2219 aluminum alloy structure for UWMAK-III.[5] UWMAK-III is a less conservative design which might, with reasonable extrapolation, push the state of the art. This subsection, therefore, includes our most speculative magnet design concepts.

It has long been recognized that an aluminum stabilizer could be attractive because of its potential lower resistivity and reduced magneto-resistance. However, aluminum has not been used because of its low yield stress of $2 \sim 4000$ psi and large resistivity increases with strain. Our decision to use an aluminum matrix conductor is based on experiments of Boom[24] and Segal[25] which are beginning to show that under some circumstances the resistivity of over-strained aluminum will not increase excessively. These experiments involve mechanically reinforced high purity aluminum wires which have been cyclically strained to values of $\varepsilon \sim 0.1\%$, see Fig. 5. Translating from RRR, residual resistivity ratio, to resistivity, the data plotted in Fig. 5 indicate that for 2000 strain cycles the resistivity of high purity aluminum may be less than $\rho_o(B=0) \simeq 1.7 \times 10^{-9}$ Ω cm which is 1/6 the OFHC copper resistivity used in previous designs. This aluminum resistivity will saturate in high fields to about 7×10^{-9} Ω cm compared to 5×10^{-8} Ω cm for copper at 8 T. (Copper does not saturate but obeys the empirical equation $\rho \sim 10^{-8}(1+B/2)\Omega$cm, where B is in tesla). We have used $\rho = 10^{-8}$ Ω cm everywhere for the aluminum stability calculations.

Worzala[26] has noted one possible reason for this newly found aluminum insensitivity to excess strain. With electron microscopy he has

seen evidence for the development of "easy glide slip planes" in the cycled samples. It is possible that easy glide slip planes at low temperature would not necessarily continue to generate new dislocation tangles with repeated strain cycling and therefore could be responsible for a saturation resistivity which is independent of strain at an unexpectedly low value of resistivity.

The difference between these findings and earlier aluminum experiments is that they dealt with unsupported samples which were strained beyond the aluminum yield point. Such samples became plastically deformed and would continue to increase in resistivity. Our experiments are realistic engineering tests of supported samples. The gross structure of a magnet must be mechanically elastic, otherwise a magnet would tear itself apart. Any conductor, copper or aluminum, in effect is bonded to the steel or alloy structure and must strain and then recover to its exact initial location according to the stress-strain characteristics of the elastic support element. Based on the present experiments 7×10^{-9} Ω cm at any field could be used for strains up to 0.1%. We design to 0.4% strain and have used $\rho = 10^{-8}$ Ω cm, which admittedly is an extrapolation of our data. Work in progress at Wisconsin will verify the exact value to be used.

The use of 2219 aluminum alloy for the structural disk provides an excellent match for the aluminum matrix conductor. There would be no contraction stresses between the conductor and solid "D" former on cool-down, which among other advantages puts a minimum shear strain on the epoxy bonding agent. This alloy was selected for its strength, ability to be welded and heat treated and its ability to be formed at a reasonable

cost. The cost and weight of the TF coil system is reduced to one half the SS-Cu cost and weight. The only penalty is that a slightly larger volume is needed since the design stress for elastic 2219 is 45,000 psi while for steel it was 60,000 psi. The somewhat greater thickness required for the aluminum is due to its lower design stress and to the greater variation in hoop stress since the thickness to radius ratio is larger. This greater thickness of the structural disk coupled with the somewhat smaller conductors permitted by the better thermal and electrical conductivity of the aluminum conductor provides more space between conductors for the supporting lands and for the clamping bolts.

In consultation with J. Davis and A. Brown[27] a manufacturing technique was developed and is described as follows. A cross section similar to that shown in Fig. 3 will be extruded from 2219 aluminum alloy in a long straight section. A piece will be cut and bent in the plane of the extrusion for the curved outer portion. Connections between the bent and straight segments of the "D" will be made by using forged transition sections, as shown in Fig. 6 . Since the extruded portions have parallel conductor grooves which are aligned the upper transition section shown in Fig. 6 will contain an angled groove pattern necessary to allow a continuous helical winding. After welding the two extrusions and the two transition sections together to form a "D" shaped disk, the disk will be heat treated to a T87 condition and then machined to size and the grooves cleaned up to accept the conductor. The insulation and placement of the conductor and the curing of the adhesive insulation would probably be accomplished best in the milling and assembly machine.

The assembly of a magnet sector is slightly different for aluminum disks as compared to stainless steel disks. When using stainless steel disks, micarta spacers and aluminum clamping bolts, the excess thermal contraction of the aluminum alloy bolts results in an increase in the clamping force on cool-down. With aluminum disks, however, the clamping force will be reduced upon cooling due to the differential excess contraction of micarta. To maintain the required clamping between disks, Belleville washers (conical disk springs) will be used at each end of each aluminum clamping bolt, see Fig. 7 . To permit these washers to be mounted in a minimum space, the conductors will be eliminated on the outer surfaces of the outer disks. Each micarta spacer will be placed over the clamping bolts which have a center to center spacing of approximately 30 cm each way. This will provide positive positioning of the spacers and well-defined cooling channels for helium.

The cross section of the assembled magnet is shown in Fig. 8 . The inner dewar wall is assembled against micarta spacers to a tight fit around the magnet. A series of reinforced epoxy struts between inner and outer dewar walls provides lateral support to the magnet, as discussed later.

VI. Magnet Safety and Protection

The problem of magnet safety and protection is addressed in this section. We consider the case in which one TF coil develops a problem which requires that its current be discharged as soon as possible.

Typically this could be caused by losing vacuum, losing helium, shorting a coil to ground, developing a local hot spot, developing an open circuit or other. It is our intention that the design of the UWMAK coils is such that the following protective scheme will be available.

1. Each TF coil is in a separate dewar so that only the bad coil needs to be discharged.

2. Normally all coils would be operated in series with one three-phase Graetz bridge power supply. In case of a fault in one coil automatic shorting switches would short out all coils individually so that the power supply would be across only the bad coil. The power supply which was set at a few volts positive to balance lead losses would be immediately switched to -10,000 volts. The 10,000 A current in the bad coil would then decay linearly to zero since a Graetz bridge provides an almost constant voltage independent of current level. In fact, the voltage rises slightly at lower currents. Thus the decay is superior to using a simple dump resistor with its exponential L/R decay time.

3. The other coils absorb the coupled flux from the discharged coil by increasing their currents, mostly in the nearest neighbors. It is important to initially design for extra current capacity and extra cooling so that the added current will not drive a TF coil normal.

4. The penalty for using this scheme is three-fold. First, every TF coil and the leads must be designated for 10 kV. Some variation of complete insulator coverage of the stainless former seems necessary. Second, the over-rated power supply would cost about $\$2 \times 10^6$, which however, adds only 1.5% to the Tokamak cryogenic costs. Third, all coils must be designed to withstand the overcurrent and unbalanced forces developed during the shutdown of one coil.

Detailed temperature rise calculations and discharge times are found below. The coupling provided by the other TF coils reduces the energy per coil which must be removed to about 20% of the per coil energy. Note also that the gross flux in the TF system changes very little due to dropping one coil, largely removing general eddy current forces and losses.

As a reference point let us consider the circuit of Fig. 9 during shutdown. Here we restrict the component to ground voltage drop to 5 kV; hence, the converter voltage is limited to 10 kV. As mentioned above , because of the shorting switches, the power supply would discharge only the faulty coil and take advantage of inductive coupling to transfer most of the energy directly to the rest of the TF magnet.

To simplify the inductance computations for UWMAK-II we take 24 circular coils of radius a = 10 m arranged to form a toroid of major radius R = 14.5 m. Each coil has 1200 turns of copper stabilized TiNb superconductor carrying 10,000 A. The inductance of the TF magnet as a whole is L = 5400 h, and the stored magnetic energy is 2.7×10^{11} J.

The self inductance of a single coil is 60 h. If a 10 kV back emf were applied to one of the coils and the current in the rest of the magnet were held fixed by an external power supply, it would take 1 minute to shut down the coil. Here 3×10^{9} J or about 1% of all the energy in the TF system would be removed by the 10 kV power supply. A smaller amount of energy would be extracted from the rest of the magnet.

By placing each individual coil in persistant mode even more energy is transferred directly from the failing coil to the rest of the TF system. Approximate values of the coil-to-coil mutual inductances were obtained using the tables of Grover.[28] The circuit equations for Fig. 9 were solved to give the current increases in coils 2 through 24, Table 2.

Under these conditions the apparent inductance of coil 1 is L_o = 48 h as compared to 60 h for the self inductance. The energy removed via coil 1 is now 2.4 x 10^9 J. When a voltage of 10 kV is applied to the failing coil, it takes 48 sec to reduce the current to zero. This is far superior to the 100 min needed to discharge all coils in series. It is even much better than an expensive scheme of having a 10 kV converter for each sector to discharge all coils together in 5 min. For the rest of our discussion we take a single coil discharge time of 1 minute and examine the adiabatic heating of that coil and the current and force changes in the rest of the TF magnet.

There are 3.2 x 10^8 g of copper in each sector. If all coils were in separate persistent circuits and the power supply did not extract energy, the failing coil would absorb 3 x 10^9 J. If this energy were uniformly distributed throughout the copper. the temperature rise would be

$$\int_{4K}^{T} c\,dT = \frac{\Delta W}{m} \simeq 10 \text{ J/g} \qquad (20)$$

$$\Rightarrow T \simeq 90 \text{ K}.$$

A more serious problem occurs when energy is deposited is a small fraction of the conductor. As an example T would exceed 300 K if the ΔW above went into less than 13% of the copper of one coil.

If a small portion of a coil is normal as in the case of a local lack of coolant, one should know the adiabatic temperature rise of that region during the 1 min "powered shutdown" described above. Various parameters are defined as follows:

$c(T)$ specific heat of OFHC copper

$\rho(T)$ electrical resistivity

D mass density

t_{dis} discharge time

$J(T) = J_{max}(1-t/t_{dis})$ current density

The rate of change of temperature with respect to time is

$$\frac{dT}{dt} = \frac{J^2\rho}{cD} . \tag{21}$$

This leads to the integral relationship

$$D \int_{4K}^{T_{max}} \frac{c}{\rho} dT = \int_{o}^{t_{dis}} J^2 dt = \frac{1}{3} J_{max}^2 t_{dis} . \tag{22}$$

For a 1.7 x 1.13 cm conductor carrying 10,000 A, J_{max} is 5210 amp/cm^2. Equation (22) was solved to give

$$T_{max} = 54 \text{ K.} \tag{23}$$

Consequently if the early stages of a fault are detected a coil could be shut down before any portion of it exceeded 54 K.

For the above technique to work it is vital to preserve the integrity of the copper stabilizer. If it were partially destroyed or

broken, the resistance and current density terms in Eq. (22) would no longer be valid and drastic temperature rises could result.

The induced current changes and lateral forces due to one coil shutdown are shown in Table 2. The coils adjacent to the failing one absorb a 26% overcurrent. Conductor safety features discussed earlier allow for an approximate doubling of current without a normal excursion, making 26% an acceptable fault condition overcurrent. If two adjacent coils such as 1 and 2 fail, the current increase in coils 3 and 24 would be $-\Delta T_3/I_1 = 0.39$, still a tolerable overcurrent.

When a TF coil is shut down very large lateral forces are produced, to the extent that special structures must be used to accommodate them. This will be discussed in the next section.

VII. Structural Design

In both UWMAK-II and III lateral support around the perimeter of each TF coil is required in order to: (1) adjust the coils to their equilibrium position, (2) to hold the coils in place during poloidal field pulsing and (3) to stabilize the coils during a catastrophic failure of one or more TF coils. The last of these situations requires the gratest amount of lateral support and is the basis for the design described here.

If one TF coil loses current then flux and energy are removed as described above. The impulsive lateral forces on all other coils are listed in Table 2 as a ratio of force to F_o. The force F_o is the nominal repulsive force between two parallel conductors, each of which

Table 2

Induced Currents in the Toroidal Field Magnets and Shell Stresses and Circumferential Motions of the Dewars Due to the Failure of Magnet Number 1

Magnet No. k	$-\frac{\Delta I_k}{\Delta I_1}$	$\frac{F_k}{F_o}$	$\frac{\Sigma F_k}{F_o}$	Lateral Compressive Shell Stress (N/cm^2)	Lateral Dewar Motion (cm)
1	-1	0	0	0	0
2 24	0.2571	1.14	1.14	6920	10.34
3 23	0.0336	0.19	1.33	8670	9.68
4 22	0.0224	0.13	1.46	8860	8.89
5 21	0.0147	0.10	1.56	9460	8.05
6 20	0.0110	0.08	1.64	9950	7.14
7 19	0.0088	0.06	1.70	10310	6.17
8 18	0.0075	0.04	1.74	10560	5.18
9 17	0.0066	0.03	1.77	10740	4.17
10 16	0.0061	0.02	1.79	10860	3.15
11 15	0.0057	0.01	1.80	10920	2.11
12 14	0.0055	0.01	1.81	10980	1.07
13	0.0054	0			0

is carrying a current I_o and spaced a distance s apart.

$$F_o = \frac{2(10^{-7})I_o^2}{s} \quad N/m \ , \tag{24}$$

where I_o is the normal operating current of 10×10^6 A per coil. Also listed in Table 2 is the summation $\sum F_k/F_o$ around the toroid which creates the compressive stresses also listed. The distortion of the toroidal field due to I dropping to zero in one TF coil causes the other 23 coils to try to snap around into a straight line solenoid. The net result is to compress support structure between all coils except for the two sides of the failed coil where the support structure might be in tension.

Our solution to this problem is shown in Fig. 10. The secondary vacuum shell between coils is also the lateral support member. The shell is provided with unidirectional slip joints so that no tensile forces can be developed between dewars. A system capable of carrying the loads in tension would require more structure and would be more costly and difficult to design. The spring-loaded slip joint would be mounted at the centerline of each shell, Fig. 10. This slip joint is provided with O-ring type seals just as are the joints between the shells and the dewars.

Since the lateral forces due to the field distortion vary inversely as the distance between magnets and this distance in turn varies almost directly with the radial distance from the central toroidal axis, the wall thickness and the reinforcing rib areas of the shell shown in Fig. 10 vary inversely as the radius. This keeps the compressive stress in the shell structure as nearly constant as possible and minimizes the lateral bending strains in the magnet.

To transmit the circumferential load from shell to shell through the inner and outer dewar walls requires that these walls carry the compressive stresses across a length of 152 cm without suffering any buckling. To accomplish this for the maximum load requires that the inner dewar wall be braced with lateral ribs spaced 1 m apart along the length of the dewar. As the dewar major radius (distance from the central axis of the toroid) decreases, the wall thickness and the rib thicknesses must be increased as was discussed for the shell thicknesses. The thickness of the outer dewar wall and its braces must be similarly varied.

The lateral loading on the dewar side walls is transmitted from the toroidal field magnets to the dewars by the fiber-reinforced epoxy struts shown in Fig. 8 . It is possible to provide struts capable of transmitting the loads produced by the failure modes but they cannot be in contact with the outer dewar wall without causing an excessive heat leak into the magnet. Therefore, ten percent of the struts are provided with a nonlinear conical spring cap as shown in Fig. 11. The remainder will be the same strut without the cap and will have a clearance of approximately 1 cm from the outer dewar wall.

The conical spring cap must be strong enough to provide the proper ordinary centering forces, must slide easily on the smooth stainless steel dewar walls during cool-down, must slide back out to larger radius with field energization, and must have sufficiently large spring constant to accommodate the lateral forces due to pulsed poloidal field coils.

The conical spring caps must not overload the struts on which they are mounted when a failure condition occurs such as the loss of one or two toroidal field magnets as previously discussed. Under this condition, the force in the conical spring cap will reach a peak and decrease slightly as all of the stand-off struts move into contact. The proposed shape of the conical spring cap is shown in Fig. 11 along with the desired load deflection curves.

The UWMAK-II and III designs accounted for a worst case of two adjacent coils losing current, which is an obvious extrapolation of the above one coil example. Two adjacent coils without current represent a more severe case than two non-adjacent coils without current. It is considered improbable that any two coils would fail simultaneously (within one minute of each other) since all coils have been designed to easily absorb a one minute pulse of extra current and the accompanying impulsive force. While it is possible to design for 3 or more adjacent coils which lose current simultaneously the extra expense for structure seems unwarranted.

VIII. Summary

We have discussed fully cryogenically stable superconducting toroidal field magnets which should operate without failures for the lifetime of a Tokamak fusion power reactor. These UWMAK studies outline an imbedded conductor design using composite conductors of TiNb superconductors in copper or aluminum stabilizer. The conductors are inserted in grooves in manufactured structural disks of stainless steel or aluminum. This method of construction allows maximum flexibility in

designing constant tension magnet shapes and provides optimum radial and lateral support for the toroidal field magnets. Individual disks can be fully tested in the operating environment before assembly into the final form.

The major concern with this type of structure is associated with a voltage breakdown during a fault condition while energy is being removed rapidly from a single magnet. Necessary design details and protection schemes are being examined in order to solve these problems. This paper introduces the general philosophy of using separate dewars, isolating problems into small sub-units, and relying heavily on mutual coupling to interrupt rapid field decay. Such protection schemes make maximum use of the inherent coupling between adjacent coils and offer promise of relieving eddy current decay problems in the remainder of the structure.

The above study illustrates that fully stable magnets using composite conductors should be engineered without major uncertainties according to straightforward scientific concepts. While subsequent designs will undoubtedly include improvements there is no reason to expect that superconductivity implies ventursome unknown TF coil performance. There is no question but that stable DC superconducting magnets will "work" based on past experience. AC effects, which were not addressed in this paper, represent new and different problems for the designer and may in fact limit rise times for future pulsed reactor magnets. At present in 1976 it does not appear that rapid pulsing, e.g., less than 1 sec rise time, would be required for large reactor systems. In this case, the above design is probably adequate without reference to AC problems.

Acknowledgements

We acknowledge the substantial contributions to the UWMAK design studies made by Y.M. Eyssa, M.A. Hilal, J.W. Lue, P.H. Sanger, H.R. Segal, I.N. Sviatoslavsky and R.L. Willig.

We also gratefully acknowledge the United States Energy Research and Development Administration and the Wisconsin Electric Utilities Research Foundation for their support of research on UWMAK-II and the Electric Power Research Institute for their support of research on UWMAK-III.

References

1. R. Clausius, Phil. Mag. 40, 122 (1870).
2. R.H. Levi, ARS Journal 32, 787 (1962).
3. J. File, R.G. Mills and G.V. Sheffield, IEEE Trans. on Nuc. Sci. NS-18, 277 (1971).
4. G.L. Kulcinski, R. Conn, et al., "UWMAK-I, A Toroidal Tokamak Power Reactor Design," Nucl. Engr. Dept. Report, UWFDM-68 (Univ. of Wis., Oct. 1974).
5. R. Conn et al., "UWMAK-III, An Advanced, Noncircular Tokamak Power Reactor Design," Nucl. Eng. Dept. Report, UWFDM-150 (Univ. of Wis., Dec., 1975).
6. W.M. Stacey, et al., "EPR Design Studies," Argonne National Lab. Report ANL-CTR-75-2 (1975).
7. R.G. Mills, ed., "A Fusion Power Plant," Princeton Plasma Physics Lab Report MATT-1050 (1974).
8. J. File and G.V. Sheffield, Proc. of the Fourth International Conference on Magnet Technology, (CONF-720908, USAEC, NTIS, Springfield, Va., 1972), p. 240.
9. S.T. Wang, J.R. Purcell, D.W. Demichele and L.R. Turner, "ANL Pure Tension TF Coil Studies," Sixth Symposium on Engineering Problems of Fusion Research, Paper A4-1 (San Diego, Nov., 1975).
10. R.W. Moses and W.C. Young, "Analytic Expressions for Magnetic Forces on Sectored Toroidal Coils," Ibid, Paper D3-4 and Nucl. Eng. Dept. Report UWFDM-143 (Univ. of Wis., 1975).
11. J. Boris and A.F. Kuckes, "Closed Expressions for the Magnetic Field in Two-Dimensional Multipole Configurations," Princeton Plasma Physics Laboratory Report MATT-473 (1966).

12. R.J. Roark and W.C. Young, Formulas for Stress and Strain, 5th ed., McGraw-Hill Book Co., 1975.

13. R. Conn et al., "UWMAK-II, A Conceptual D-T Fueled, Helium Cooled, Tokamak Fusion Power Reactor Design," Nucl. Eng. Dept. Report UWFDM-112 (Univ. of Wis., Oct., 1975).

14. A.R. Kantrowitz and Z.J.J. Stekly, Appl. Phys. Letters, 6:56 (1965).

15. D.N. Cornish, "Superconducting Coils Using Stranded Cables," U.K. Atomic Energy Authority Report No. CLM-P83 (1965).

16. Z.J.J. Stekly and J.L. Zar, IEEE Trans. on Nuc. Sci., NS-12:367 (1965). Z.J.J. Stekly, J. Appl. Phys. 37:324 (1966).

17. C.N. Whetstone, G.G. Chase, J.W. Raymond, J.B. Vetrano, R.W. Boom, A.G. Prodell and H.A. Worwetz, IEEE Trans. on Magnetics MAG-2:307 (1966).

C.N. Whetstone and R.W. Boom, Advances in Cryogenic Engineering, 13:68 (1968).

18. D.N. Cornish, J. Zbasnik and H.E. Pattee, Sixth Symposium on Engineering Problems of Fusion Research, paper B1-3 (San Diego, 1975). R. Nelson, D. Cornish, J. Zbasnik, S. Sackett and C. Taylor, Ibid, paper A3-13 (1975).

19. R.W. Boom, R.W. Conn and J.W. Lue, "Apparent Difficulties Associated with High Magnetic Field Large Tokamak Power Reactor Designs," Ibid, paper C2-8 (1975) and Nucl. Eng. Dept. Report UWFDM-146 (Univ. of Wis., 1975).

20. G.L. Kulcinski and J.R. Young, International Conference on Radiation and Tritium Technology for Fusion-Reactors, Gatlinburg (1975) and Nucl. Eng. Dept. Report UWFDM-140 (Univ. of Wis., 1975).

21. M.A. Hilal and R.W. Boom, "Cryogenically Stable conductors for Toroidal Fusion Reactor Magnets," Sixth Symposium on Engineering Problems of Fusion Research, paper B1-4 (San Diego, 1975) and Univ. of Wis. Report UWFDM-144 (1975).

22. K. Wohlleben, Jour. Low Temp. Phys., Vol. 13, No. 3/4, p. 269 (1973).

23. J. Purcell, H. Desportes and D. Jones, "Superconducting Magnet for the 15 foot NAL Bubble Chamber," Argonne National Lab Report ANL/HEP 7215 (1973).

24. R.W. Boom, P. Brown and F.J. Worzala, Bull. Am. Phys. Soc. 17, 1195 (1972).

25. H.R. Segal and T.G. Richard, Adv. in Cryogenic Engineering, Kingston, Ont. (1975), to be published.

26. F.J. Worzala, private communication.

27. J. Davis and A. Brown, McDonnell-Douglas Corp., private communication.

28. F.W. Grover, Inductor Calculations (Dover Pub. Inc., N.Y., 1946).

List of Figure Captions

Fig. 1. Side view of a constant tension D coil.

Fig. 2. Toroidal cross section as viewed from above.

Fig. 3. Cross section of the conductor and structural disc.

Fig. 4. Superconductor current density design curves.

Fig. 5. Change in the residual resistance ratio with the number of strain cycles to 0.1% strain for reinforced elastic samples. Test conditions: 4.2 K and B = 0.

Fig. 6. Forged transition section for toroidal field magnet discs.

Fig. 7. Lateral load bearing epoxy strut.

Fig. 8. Cross section of toroidal field magnet.

Fig. 9. TF coils shown shorted for rapid discharge of faulted coil.

Fig. 10. Secondary vacuum shell and lateral support.

Fig. 11. Load deflection curve for the conical spring cap.

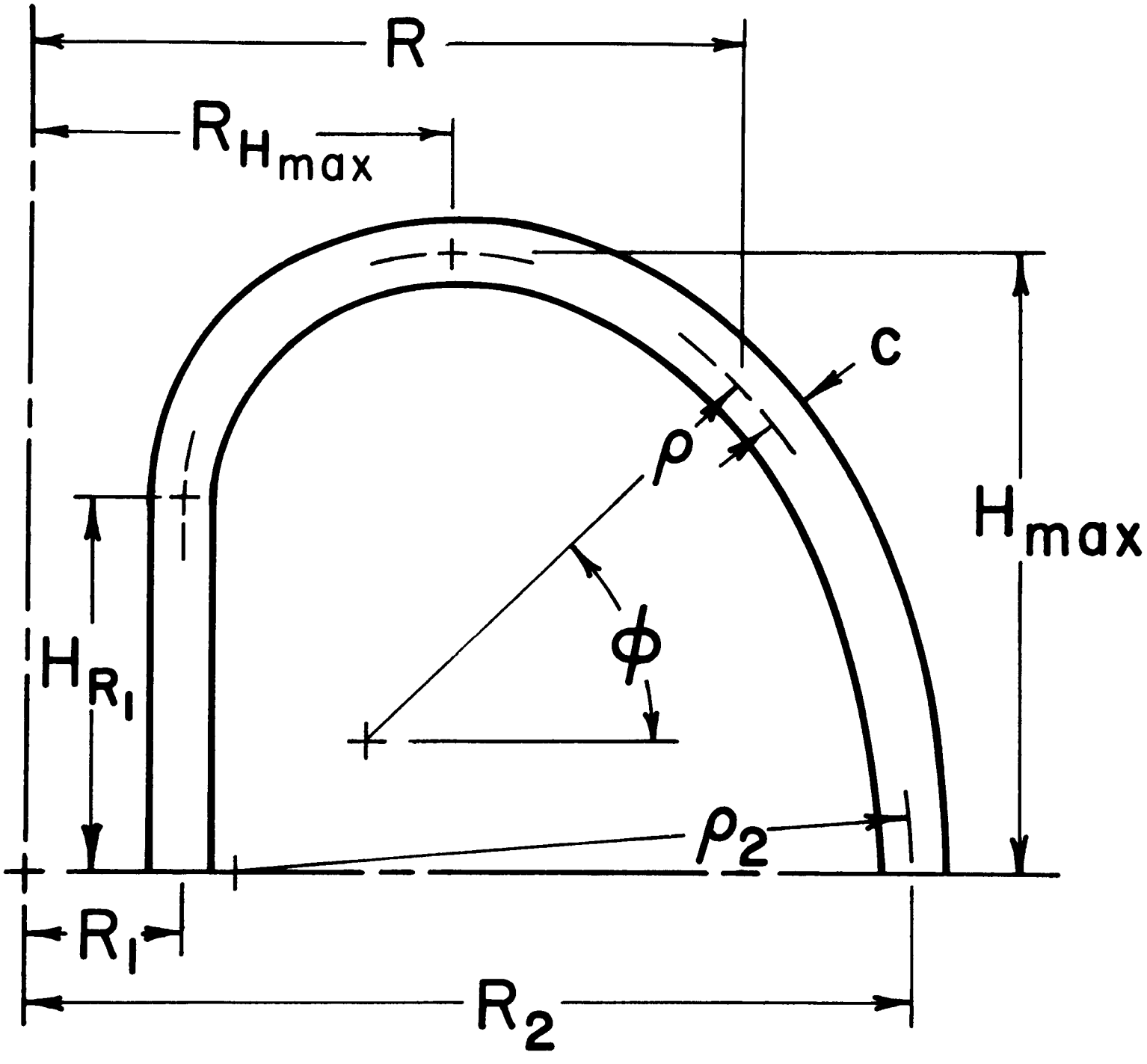
R
$R_{H_{max}}$
c
ρ
H_{max}
ϕ
H_{R_1}
ρ_2
R_1
R_2

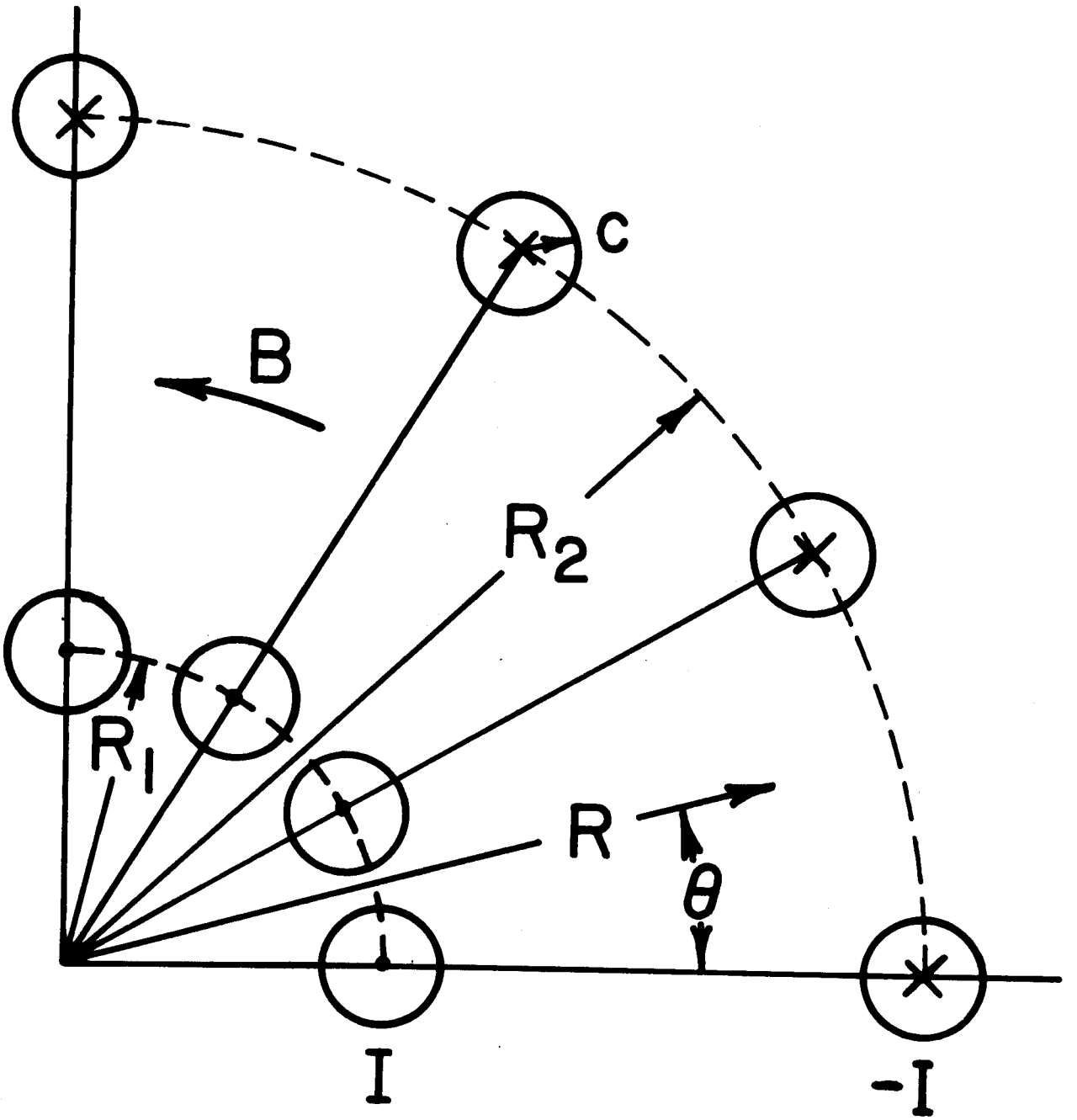

FIGURE 2

DETAIL OF UWMAK-II T.F. MAGNET CROSS SECTION

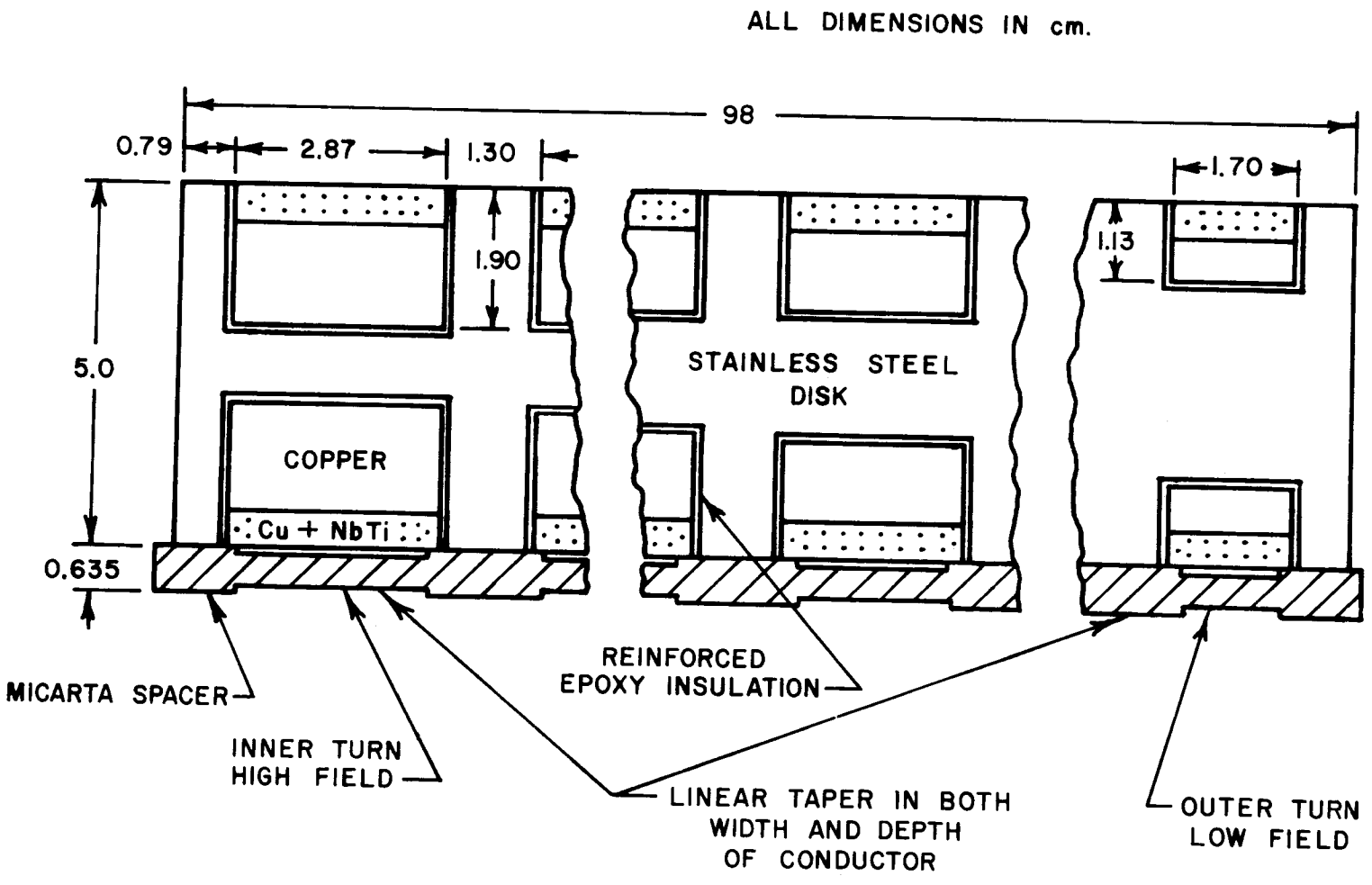

FIGURE 3

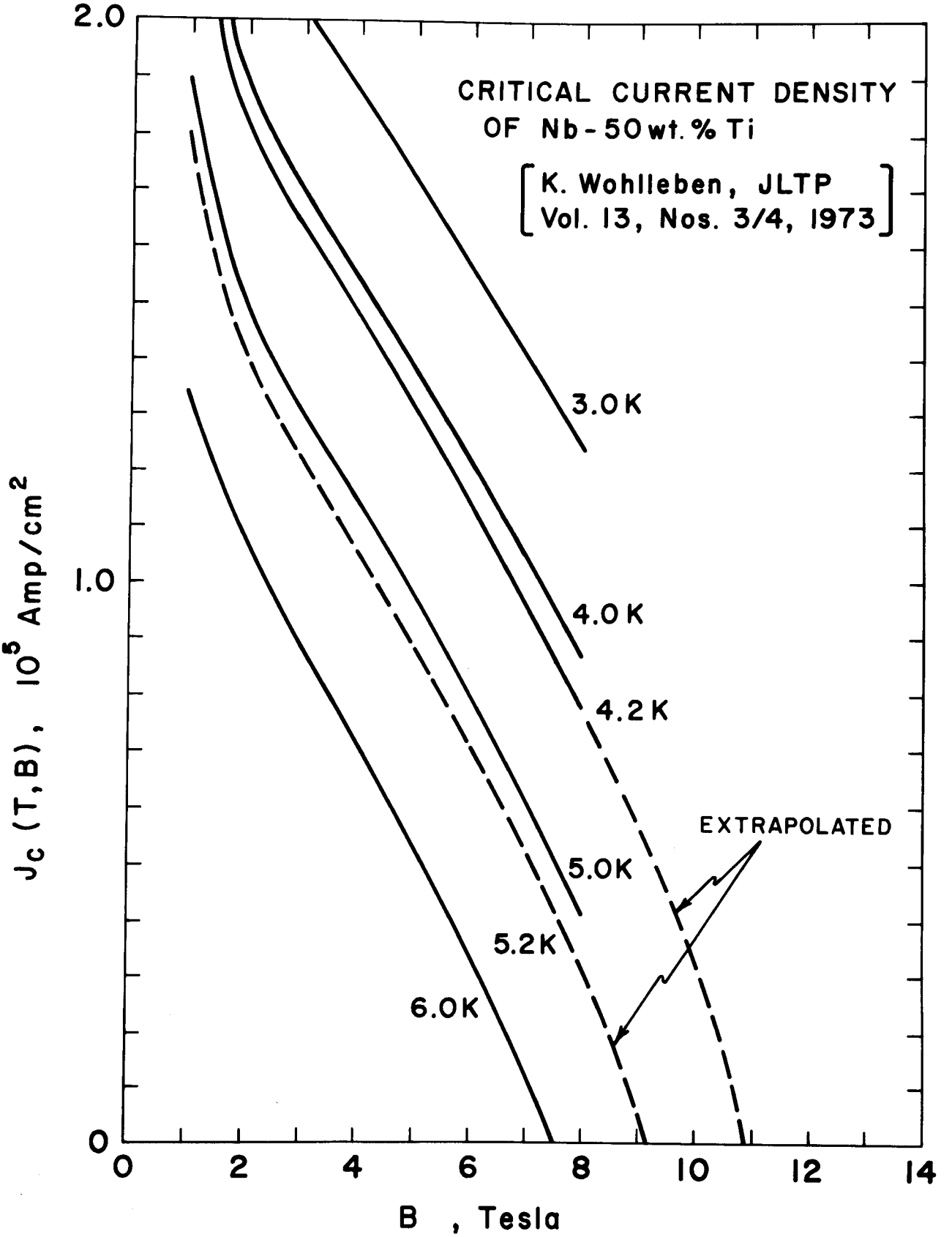
CRITICAL CURRENT DENSITY
OF Nb-50 wt.% Ti
[K. Wohlleben, JLTP
Vol. 13, Nos. 3/4, 1973]
3.0K
4.0K
4.2K
5.0K
5.2K
6.0K
EXTRAPOLATED
J_c (T,B), 10^5 Amp/cm^2
B , Tesla
0
1.0
2.0
0
2
4
6
8
10
12
14

FIGURE 4

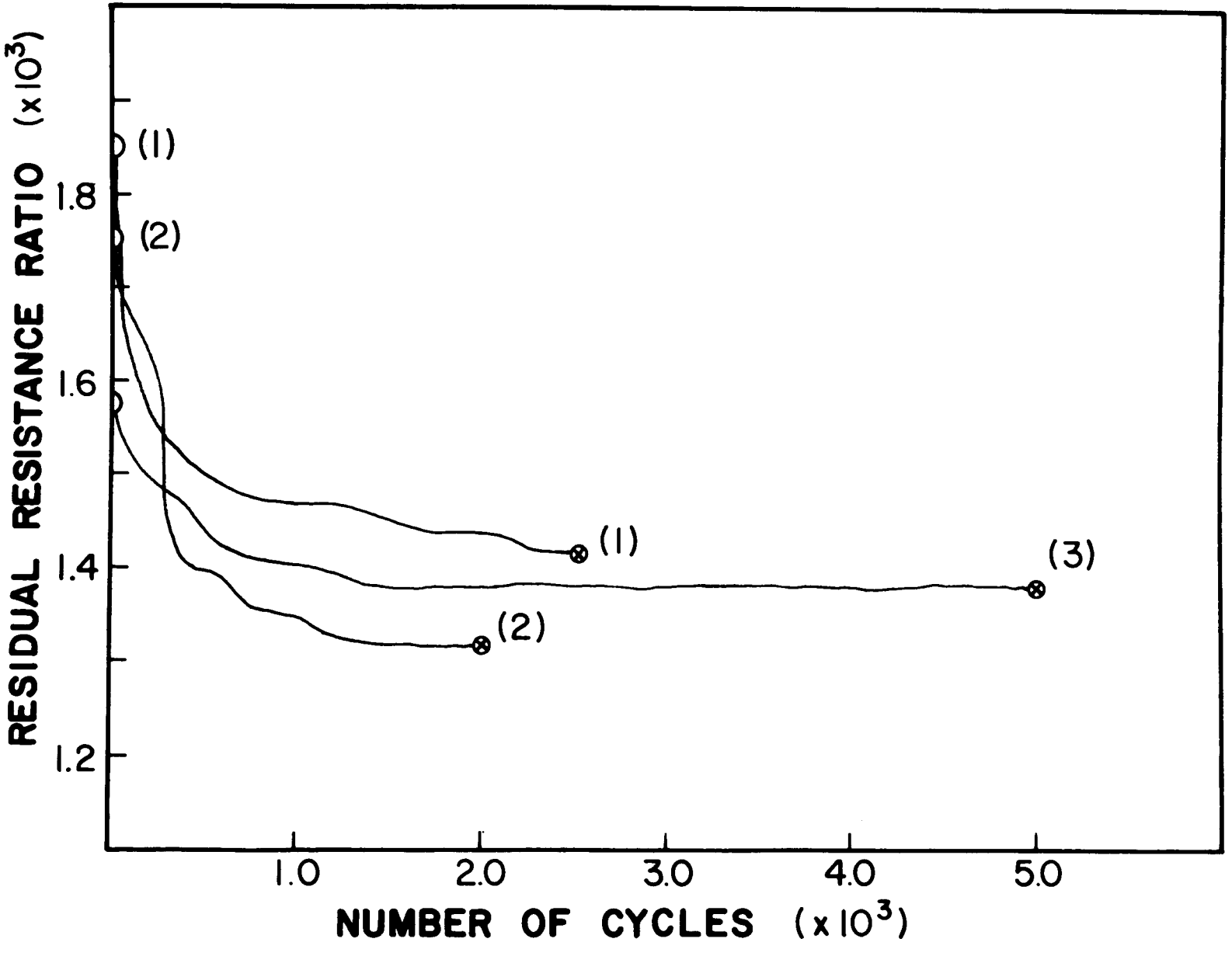
RESIDUAL RESISTANCE RATIO (x10³)
1.8
1.6
1.4
1.2
(1)
(2)
(1)
(2)
(3)
1.0
2.0
3.0
4.0
5.0
NUMBER OF CYCLES (x10³)

FIGURE 5

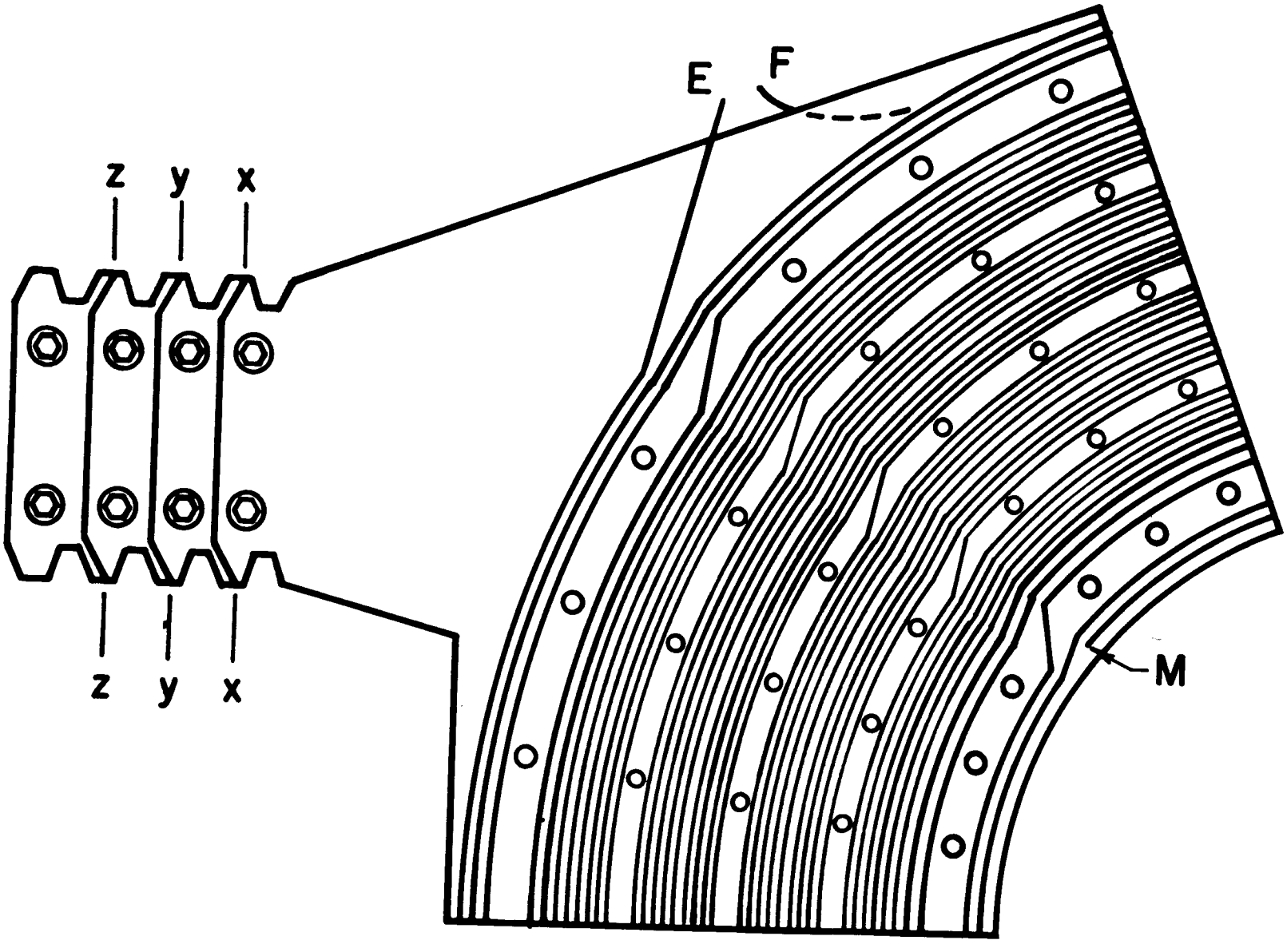

FIGURE 6

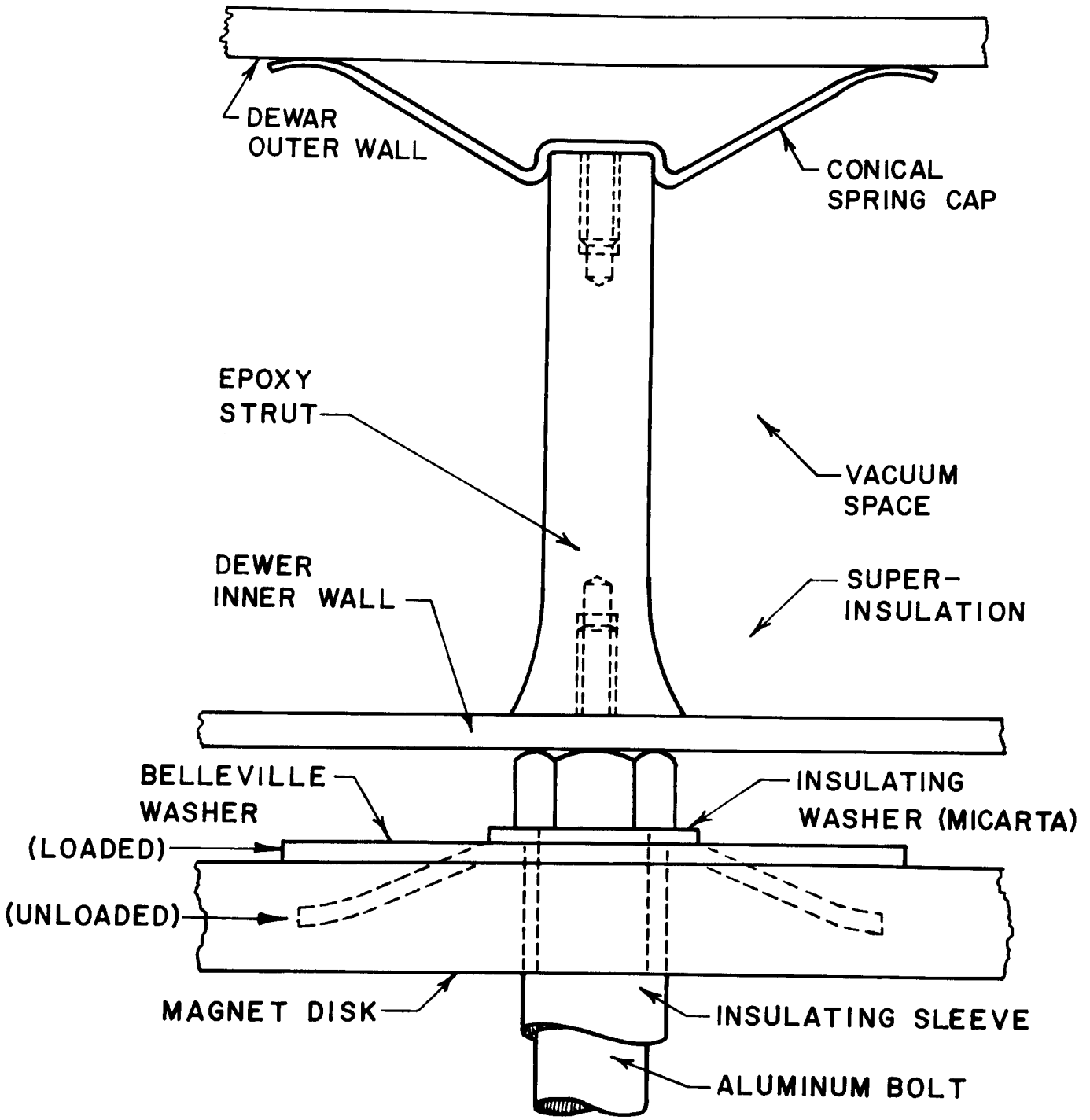
DEWAR
OUTER WALL
CONICAL
SPRING CAP
EPOXY
STRUT
VACUUM
SPACE
DEWER
INNER WALL
SUPER-
INSULATION
BELLEVILLE
WASHER
INSULATING
WASHER (MICARTA)
(LOADED)
(UNLOADED)
MAGNET DISK
INSULATING SLEEVE
ALUMINUM BOLT

FIGURE 7

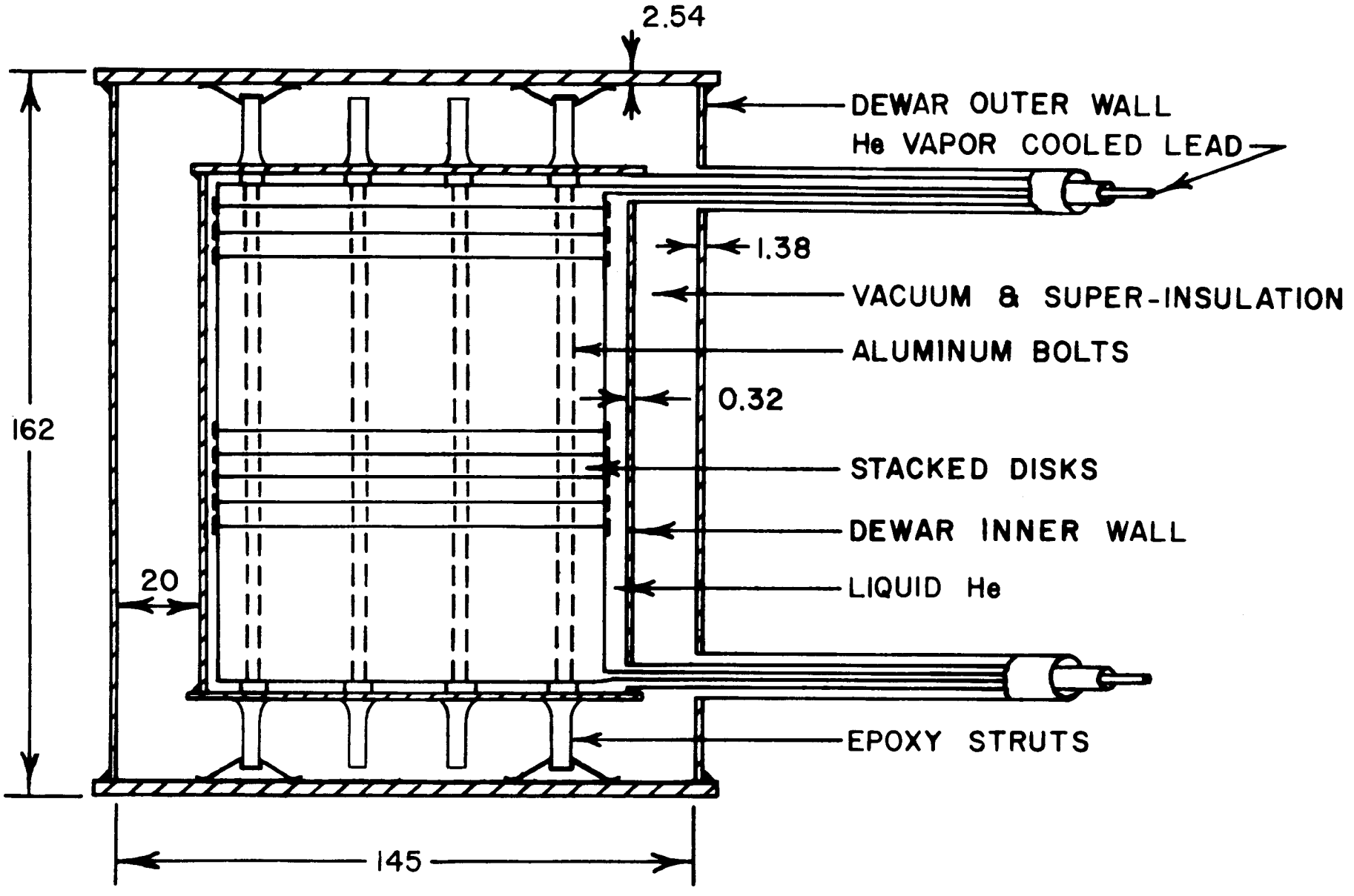

ALL DIMENSIONS IN cm.

FIGURE 8

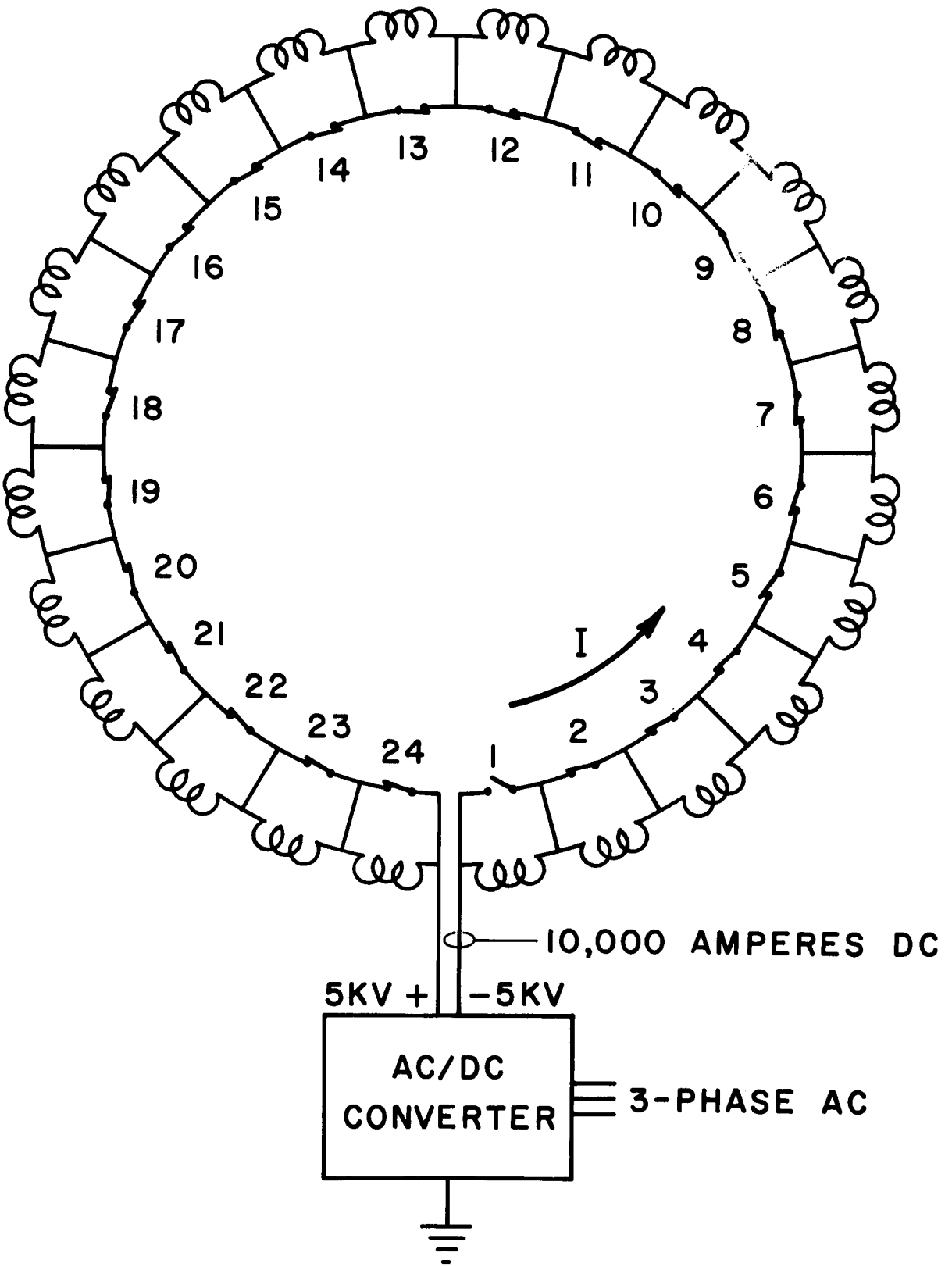
1
2
3
4
5
6
7
8
9
10
11
12
13
14
15
16
17
18
19
20
21
22
23
24
I
10,000 AMPERES DC
5KV +
-5KV
AC/DC
CONVERTER
3-PHASE AC

FIGURE 9

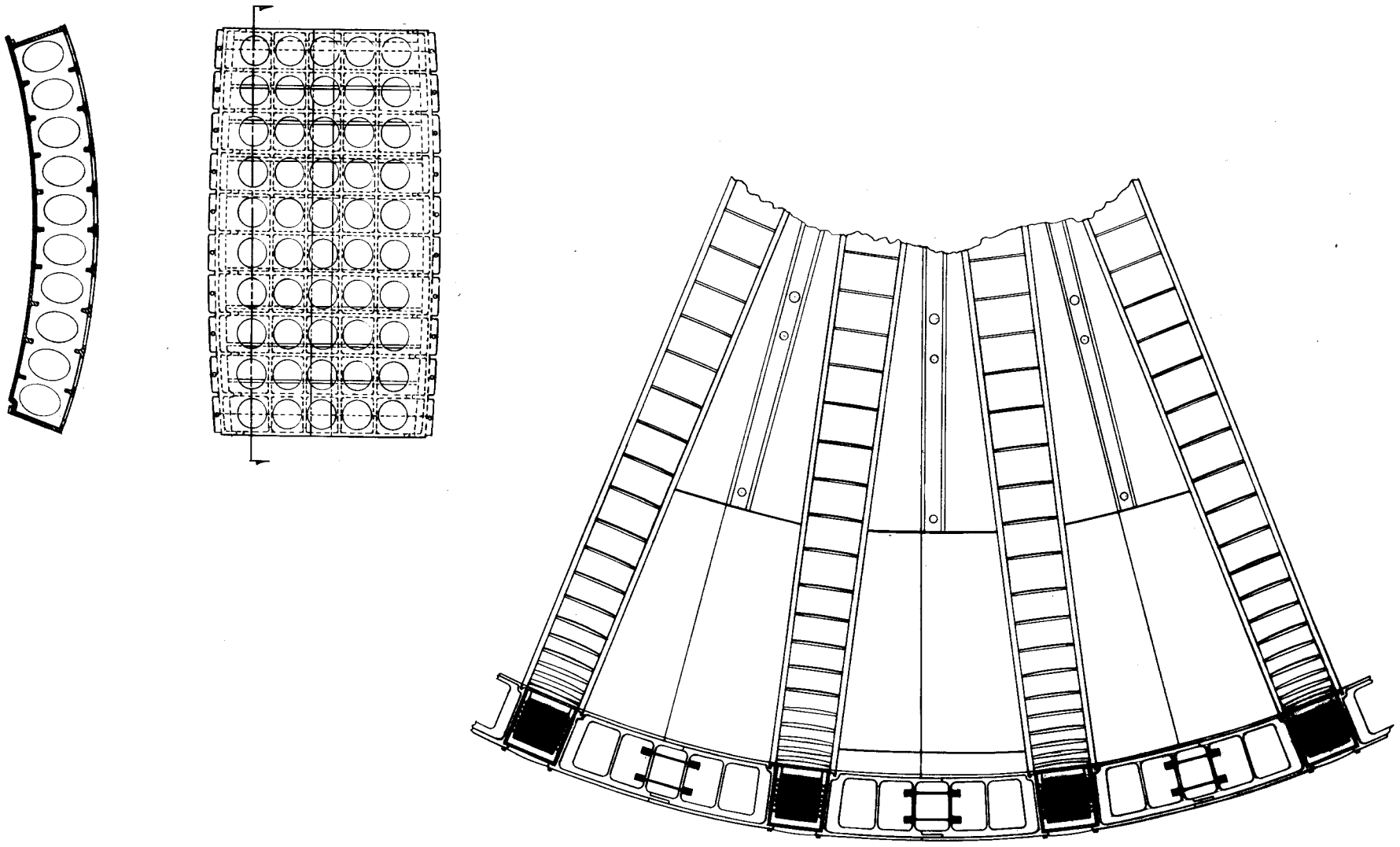

FIGURE 10

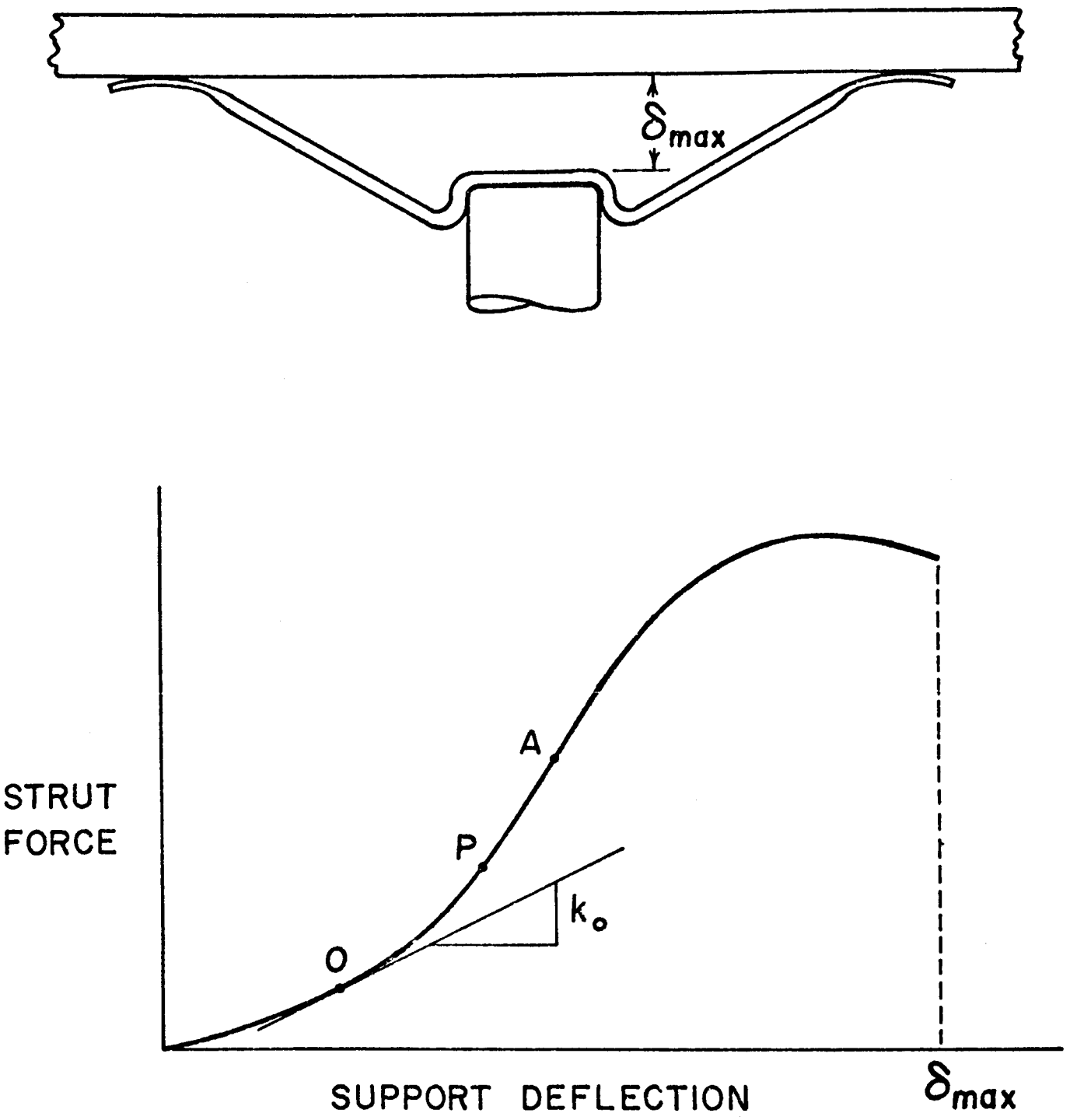

FIGURE 11